# CONTINUOUS LIDAR MEASUREMENTS OF STRATOSPHERIC AEROSOLS AND OZONE AFTER THE PINATUBO ERUPTION. PART I: DIAL OZONE RETRIEVAL IN PRESENCE OF STRATOSPHERIC AEROSOL LAYERS

Alfonso D'Altorio[1], Fabrizio Masci[2], Vincenzo Rizi[2] Guido Visconti[1], Enzo Boschi[2]

Abstract. We report stratospheric DIAL (DIfferential Absorption Lidar) ozone observations in presence of large amount of volcanic aerosols, which strongly affect the inversion of the backscattering signals. The retrieval method is based on the use of three wavelengths, two from the $O_3$ DIAL (308 and 351nm) and a third one from an aerosol lidar (589nm) operated at the same site (L'Aquila, Italy; 42°N,13°E). For each measurement session the relationships between the backscattering ratios at different wavelengths are fitted with an appropriate size distribution of the aerosols. The aerosol optical properties determined with this procedure allow to correct the ozone profiles. The ozone data are compared whenever possible with balloon ozonesonde measurements taken at S.Pietro Capofiume (Italy, 45°N, 11°E) or Hohenpeissenberg (Germany, 48°N, 11°E) and they generally show a good agreement. The ozone profiles can be retrieved with an indetermination that, within the aerosol layer, ranges between ±15 to ±35%. A systematic intercomparison is reported with data of other stations to assess the reliability of the method.

## Introduction

The eruptions of Mt.Pinatubo (15°N, 120°E) in the Philippine Islands during the period 12-16 June 1991, produced a large aerosol load in the stratosphere. An enhanced aerosol layer could play an important role in activating the heterogeneous chemistry in the middle latitude stratosphere, as shown by Hofmann and Solomon (1989), that could result in a large ozone loss. The eruption of Pinatubo may offer an opportunity to test this theory, so that a continuous monitoring of stratospheric aerosols and ozone content is needed.

The lidar station of the University of L'Aquila (SLAQ, located 42°N, 13°E and 700m a.s.l.) includes an aerosol lidar system (589nm) and, since July 1991, a DIAL (DIfferential Absorption Lidar) facility (308 and 351nm). Both systems have been described in D'Altorio and Visconti (1983) and D'Altorio et al. (1992). In the DIAL measurements, the enhanced scattering in the altitude range of the particle layer and the transmission loss due to aerosol extinction has to be removed from the retrieved ozone profiles; this can be done if the wavelength dependence of aerosol scattering and extinction cross sections are known. Several methods to estimate the correction have been proposed in the literature (i.e.

[1] Dipartimento di Fisica Università degli Studi - L'Aquila
[2] Istituto Nazionale di Geofisica

Browell et al., 1985, D'Altorio et al., 1992), and they all need to start from assumptions about the wavelength dependence of the aerosol backscattering and extinction coefficients.

In this paper we present a new algorithm to correct DIAL ozone profiles; this method enables us to obtain the aerosol optical properties directly from the observations. The algorithm uses the lidar signals at three wavelengths ($\lambda$=308,351,589nm) obtained with our systems during a standard session of measurements.

## The aerosol backscattering ratios

The backscattering ratio is defined as $R_\lambda = 1 + \beta_\lambda^a/\beta_\lambda^R$. The dependence from the altitude is implicit. $\beta_\lambda^R$ and $\beta_\lambda^a$ are respectively the molecular and aerosol backscattering coefficients (Bohren and Huffman, 1983). The calculation of $R_\lambda$'s from the lidar signals are essentially obtained with an iterative version of the method outlined by Russell et al. (1979); this algorithm enables to adjust iteratively for the transmission loss due to aerosol extinction. The nearest ozone, pressure and temperature sounding obtained at S.Pietro Capofiume, Bologna, Italy (SPCF) or Hohenpeissenberg, Germany (HOH), respectively 300km and 600km north of our station, are used to calibrate the lidar signals. $R_\lambda$'s are normalized to 1.0 in a region well above the aerosol layer (usually in an altitude range higher than 30km). The correction of $R_\lambda$'s for the effect of the aerosol extinction requires the aerosol extinction to backscattering ratio ($C_\lambda$) to be known. As initial guess we have used the same values of $C_\lambda$'s for each session of measurements; sensitivity tests have shown that $R_\lambda$'s change within a few percent even for large variations of the extinction to backscattering ratios. The first estimation of $R_\lambda$'s is used to evaluate the aerosol optical properties (i.e. $C_\lambda$, see the next paragraph). With this new values for $C_\lambda$ the backscattering ratios are further iterated but in any case they show a very little change from the first determinations. In Fig.1 a few examples of retrieved $R_\lambda$ are shown with the associated errors. These uncertainties ($\Delta R_\lambda$) have been determined according to the analysis given in Russell et al. (1979): in a standard session of measurements $\Delta R_\lambda/R_\lambda$ ranges from ±7 to ±15% for 589nm, from ±5 to ±10% for 351nm and from ±10 to ±15% for 308nm.

## Retrieval of the aerosol optical properties

The Pinatubo cloud is likely constituted of spherical sulfate aerosol particles (Sheridan et al., 1992). If we assume that for each session of measurements the observed aerosols have constant size distribution and index of refraction within the aerosol layer (from 15 to 25km), the pairs of ($R_\lambda - 1$) can be correlated by the following relationship:

$$(R_{\lambda_i} - 1) = A_{\lambda_i,\lambda_j}^{obs} (R_{\lambda_j} - 1) \qquad (1)$$
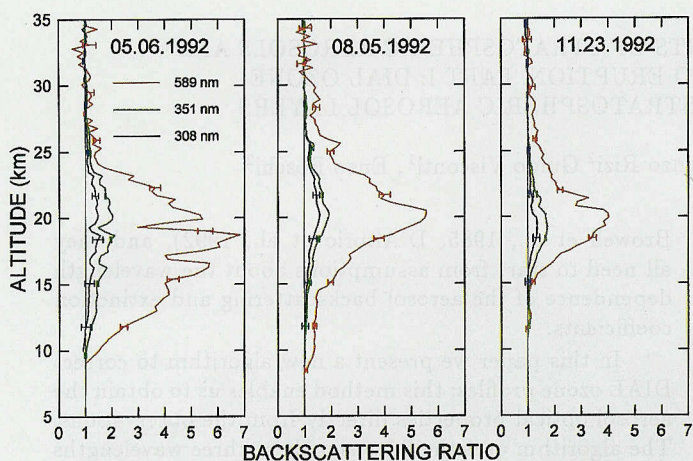
Fig.1. The figure shows the backscattering ratios corrected for aerosol extinction and ozone absorption at 308, 351 and 589nm wavelengths. The error bars on the retrieved values of $R_\lambda$ show $1\sigma$ standard deviation. The data refer to 3 different session of measurements taken at SLAQ: May 6, August 5 and November 23, 1992.

According to the Mie scattering theory, the estimate of $A_{\lambda_i,\lambda_j}^{obs}$ is:

$$A_{\lambda_i,\lambda_j} = \frac{\beta_{\lambda_i}^a}{\beta_{\lambda_j}^a} \left( \frac{\lambda_i^{\alpha(\lambda_i)}}{\lambda_j^{\alpha(\lambda_j)}} \right) \qquad (2)$$

with $i \neq j$ and $i,j = 308, 351, 589$nm, and $\alpha(\lambda_i) = (3.916 + 0.074\lambda_i + 0.05/\lambda_i)$. The dependence of the backscattering coefficients from the size distribution and the aerosol index of refraction is implicit. The set of aerosol backscattering ratios measured at 308, 351 and 589nm can be fitted to Eq.(1). In Fig.2 an example of such correlations is shown (for May 6, 1992 measurements). The slopes of the different curves constitute the observed $A_{\lambda_i,\lambda_j}^{obs}$ coefficients. These coefficients are calculated using a linear least squares fit and they are usually determined with an error ranging between $\pm5\%$ and $\pm15\%$.

We assume a log-normal unimodal size distribution for the aerosol particles, whose parameters are N, the
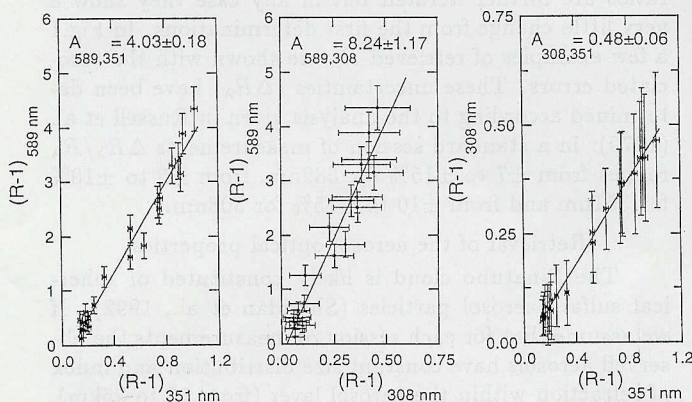


Fig.2. Plots of the relationship between the backscattering mixing ratios at the different pairs of wavelengths available at SLAQ. The data refer to May 6, 1992. The slopes are reported with the associate standard deviations.

particle number density, $r_o$, the mode radius and $\sigma$, the dispersion. Since $A_{\lambda_i,\lambda_j}^{obs}$ is independent from the aerosol number density then the parameters of our aerosol model are the index of refraction, the mode radius and dispersion of the size distribution. The assumed aerosol size distribution must be considered as an equivalent size distribution, in the sense that, as the real distribution, it leads to the same ratio between the backscattering coefficients. The model parameters can be retrieved by minimizing in the least squares sense the differences between $A_{\lambda_i,\lambda_j}^{obs}$ and the estimate (Eq.(2)), which is calculated by changing $r_o$, $\sigma$:

$$\chi = \left[ \sum_{i,j} \left( \frac{A_{\lambda_i,\lambda_j} - A_{\lambda_i,\lambda_j}^{obs}}{A_{\lambda_i,\lambda_j}^{obs}} \right)^2 \right]^{1/2} \qquad (3)$$

The aerosol index of the refraction ($m_{\lambda_i}$) is calculated from the atmospheric temperature and humidity (Russell and Hamill, 1984). Considering the temperature profiles available from SPCF or HOH balloon soundings and keeping constant the $H_2O$ partial pressure (3-6ppmv), the acid weight fraction of sulfuric solution droplets at equilibrium is estimated to change between 65% and 70%, in 15-25km range. The indices of refraction are reported in Tab.1.

In order to find the minimum of $\chi$, the mode radius-dispersion space has to be scanned; we have assumed that $r_o$ can change from $0.01\mu m$ to $1.0\mu m$ in steps of $0.01\mu m$ and $\sigma$ from 1.10 to 2.60 in steps of 0.01. The Mie efficiency factors needed for the evaluation of $\beta_{\lambda_i}^a$ and of the extinction coefficients ($k_{\lambda_i}^a$) have been calculated using the routines given by Bohren and Huffman (1983), over a large radius range (from $0.001\mu m$ to $100\mu m$), densely scanned. In the least squares calculation the model parameters are achieved when $\chi$ is less than

$$\frac{\Delta A}{A} = \left[ \sum_{i,j} \left( \frac{\Delta A_{\lambda_i,\lambda_j}^{obs}}{A_{\lambda_i,\lambda_j}^{obs}} \right)^2 \right]^{1/2} \qquad (4)$$

where $\Delta A_{\lambda_i,\lambda_j}^{obs}$'s are the standard deviations of the $A_{\lambda_i,\lambda_j}^{obs}$ coefficients. For such cases the mode radius and the dispersion of the equivalent size distribution constitute the results. Then $\beta_{\lambda_i}^a$, $k_{\lambda_i}^a$ and $C_\lambda$ ($=k_{\lambda_i}^a/\beta_{\lambda_i}^a$) are known. On the other hand $\Delta A_{\lambda_i,\lambda_j}^{obs}$'s also determine a precision limit for $\chi$ in Eq.(3) ($\Delta\chi = \frac{\Delta A}{A}$). This deviation reflects on the retrieved model parameters ($r_o$ and $\sigma$), in the sense that the least squares minimum ($\chi_{min} \pm \Delta\chi$) can be achieved for a set of points in $r_o$ - $\sigma$ space. Then, the representative parameters are the values of $r_o$ and $\sigma$ averaged over this set of points and with associated standard deviations ($\Delta r_o$ and $\Delta\sigma$). Typically $\Delta r_o/r_o$ ranges between $\pm20$ and $\pm40\%$, and $\Delta\sigma/\sigma$ between $\pm15\%$ and $\pm20\%$. The particles fall in a region of space defined by index of

Tab.1 The indices of refraction corresponding to the wavelengths available at SLAQ for sulfuric acid solution particles at stratospheric temperature with acid weight percentage in [65%,70%] interval. The imaginary part is less than $10^{-7}$ (Livingston J., private communication, 1993).

| $\lambda$ (nm) | 308 | 351 | 589 |
|---|---|---|---|
| $m(\lambda)$ | $1.49\pm0.01$ | $1.47\pm0.01$ | $1.44\pm0.01$ |

refraction and particle size parameters, where the $C_\lambda$'s are relatively less sensitive to those parameters (Evans, 1988). As a consequence the $C_\lambda$ are determined with an uncertainty ranging between $\pm 10$ and $\pm 30\%$. We refer to a companion paper (D'Altorio et al., 1993) for the details about the particle size distributions and related quantities.

### The ozone profile retrieval

Taking the derivative of the logarithm of the ratio between the DIAL signals (308 and 351nm) and including in $n_{O_3}^o$ the aerosol independent terms (i.e. Pelon and Megie, 1982), the corrected ozone profile is:

$$n_{O_3} = n_{O_3}^o - \frac{1}{(\sigma_{on} - \sigma_{off})} \times \qquad (5)$$

$$\times \left\{ \left( C_{on} A_{on,off} \frac{\lambda_{off}^{\alpha(\lambda_{off})}}{\lambda_{on}^{\alpha(\lambda_{on})}} - C_{off} \right) \beta_{off}^R (R_{off} - 1) + \quad (5a) \right.$$

$$\left. + \frac{d}{dz} \left[ ln \left( \frac{R_{off}}{1 + A_{on,off}(R_{off} - 1)} \right) \right] \right\} \qquad (5b)$$

The subscripts on and off indicate respectively the 308 and 351nm DIAL wavelengths. $\sigma_{on}$ and $\sigma_{off}$ are the ozone absorption cross sections. The aerosol disturbance to the DIAL ozone profile is made up by two terms, one from particle backscattering ((5b) in Eq.(5)) and the other from the aerosol extinction ((5a) in Eq.(5)). The former is more relevant within the aerosol layer than the latter, which contribute to the ozone number density in the altitudes above the layer.

Eq.(5) is used to retrieve the corrected ozone profile for each measurement session and examples are shown in Fig.3 for the same days of Fig.1. The indetermination due to the correction procedure and to the systematic and statistical errors in the standard treatment of ozone DIAL signals are also reported in Fig.3. In the aerosol layer the standard deviation of the ozone number density reaches a maximum which usually ranges within $\pm 15$ to



Fig.4. Percentage differences as a function of altitude and time between SLAQ measurements and HOH ozonesondes for the period November 1991-March 1992. Only the observations in coincidence ($\pm 1$ day) have been used to evaluate the deviations. The solid and dashed lines refer respectively to positive and negative values.

$\pm 35\%$. The red lines in Fig.3 refer to the ozone profiles evaluated from Eq.(5) using $A_{on,off}$, $C_{off}$ and $C_{on}$ determined from the time and altitude average of aerosol size distributions measured at Laramie (41°N), Wyoming (Deshler et al., 1993). Large differences between those DIAL ozone profiles and the balloon soundings can be observed within aerosol layers. This may be due to the spatial uncorrelation of aerosol and ozone measurements. In Fig.4 the difference between the number densities measured with the DIAL technique at SLAQ and those obtained by ozonesondes at HOH are reported. These differences can not be entirely ascribed to the method, in fact they may also be due to ozone variability between the two sites. The comparison between coincident balloon ozone soundings taken at HOH and SPCF shows differences up to $\pm 20\%$ both in lower and high stratosphere. As a further confirmation that our method gives satisfactory results we show in Fig.5 the ozone column amounts between 17.5 and 27.5km as calculated at our
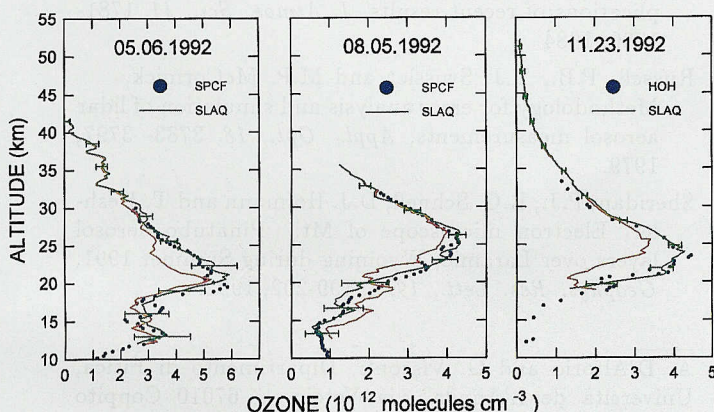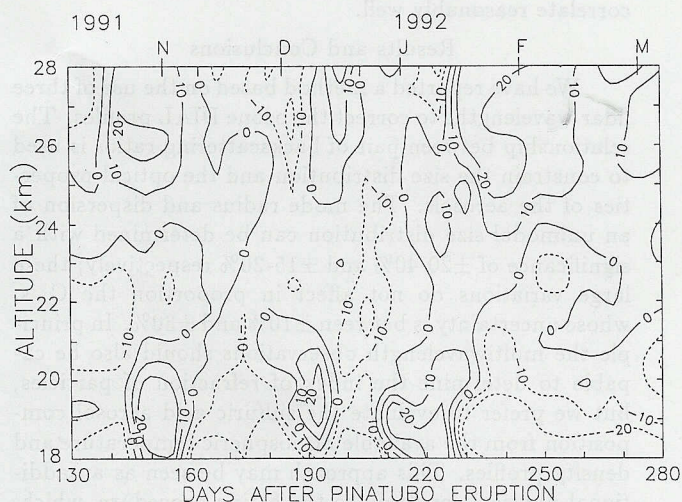


Fig.3. The recovered ozone profiles (green lines) are compared to the balloon data (blue dots) for the same days of Fig.1. Error bars indicate $1\sigma$ standard deviation on the ozone density; the indetermination also include the errors propagating through the retrieval procedure (see text for details). The red lines reproduce the ozone profiles retrieved using the size distributions reported by Deshler et al., (1993). Notice the large discrepancies between such ozone profiles and ozonesonde data.
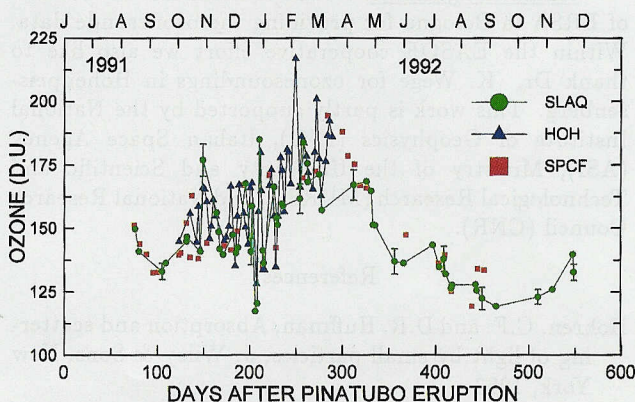


Fig.5. The time series of the partial ozone columns, as observed at SLAQ, HOH and SPCF, are shown in 17.5-27.5km altitude range. The indetermination ($1\sigma$ standard deviation) on SLAQ data are also shown.

site by integrating the retrieved ozone profiles, and the comparison with the balloon data shows that the results correlate reasonably well.

### Results and Conclusions

We have reported a method based on the use of three lidar wavelengths to correct the ozone DIAL profiles. The relationship between pair of backscattering ratios is used to constrain the size distribution and the optical properties of the aerosols. The mode radius and dispersion of an unimodal size distribution can be determined with a significance of $\pm20$-40% and $\pm15$-20% respectively; these large variations do not affect in proportion the $C_\lambda$'s, whose uncertainty is between $\pm10\%$ and $\pm30\%$. In principle the multiwavelength observations should also be capable to determine the index of refraction of particles, but we prefer to evaluate the sulfuric acid aerosol composition from the available atmospheric temperature and density profiles. This approach may be seen as an additional physical constrain to the fitting procedure, which, in such embedding, should need only two wavelengths. However retaining the use of three wavelengths adds more statistical significance to the fitting algorithm.

Comparison between our results and similar data obtained with ozonesondes indicate an agreement which is consistent with the uncertainties of the methods. Notice however that because of the large distance (several hundred km) some of these difference may be ascribed to ozone variability. Correlation between ozone column amounts measured at the three site is a further proof of the validity of our method.

Some advantages of our 3-wavelengths approach may be inferred by comparing the retrieved ozone profiles with those obtained using aerosol properties determined by balloonborne measurements (Deshler et al., 1993). In the latter case large discrepancies may be observed with respect to ozonesonde data. These can be attributed to the lack of correlation in both time and space between aerosol samplings and ozone measurements.

Considering the uncertainties connected to the retrieval procedure and the short length of the data record, it is not possible to infer any long term trend in the total ozone or local variations in the profiles. However a qualitative analysis of the data shown in Fig.5 would indicate a slightly decreasing trend consistent with recent report (Gleason et al., 1993).

### References

Bohren, C.F. and D.R. Huffman, Absorption and scattering of light by small particles, J. Wiley & Sons, New York, 1983.

Browell, E.V., S. Ismail and S.T. Shipley, Ultraviolet DIAL measurements of $O_3$ profiles in regions of spatially inhomogeneous aerosols, Appl. Optics, 24, 2827-2836, 1985.

D'Altorio, A., F. Masci, G. Visconti, V. Rizi and E. Boschi, Stratospheric aerosol and ozone lidar measurements after the Pinatubo eruption, Geophys. Res. Lett., 19, 393-396, 1992.

D'Altorio, A., F. Masci, V. Rizi, G. Visconti and M. Verdecchia, Continuous lidar measurements of stratospheric aerosols and ozone after the Pinatubo eruption. PART II: Time evolution of ozone profiles and of aerosol properties, Geophys. Res. Lett., this issue, 1993.

D'Altorio, A. and G. Visconti, Lidar Observations of dust layers transience in the stratosphere following the El Chichòn volcanic eruption, Geophys. Res. Lett., 10, 27-30, 1983.

Deshler, T, B.J. Johnson and W.R. Rozier, Balloonborne measurements of Pinatubo aerosol during 1991 and 1992 at 41°N: vertical profiles, size distribution and volatility, Geophys. Res. Lett., 20, 1435-1438, 1993.

Evans, B.T.N., Sensitivity of the backscatter/extinction ratio to changes in aerosol properties: implications for lidar, Appl. Optics, 27, 3299-3304, 1988.

Gleason, J.K. P.K. Bhartia, J.R. Herman, R. McPeters, P. Newman, R.S. Stolarski, L. Flynn, G. Labow, D. Larko, C. Seftor, C. Wellemeyer, W.D. Komhyr, A.J. Miller and W. Planet, Record low global ozone in 1992, Science, 260, 523-526, 1993.

Hofmann, D.J. and S. Solomon, Ozone destruction through heterogeneous chemistry following the eruption of El Chichón, J. Geophys. Res., 94, 5029-5041, 1989.

Larsen, N., Backscatter measurements from Thule EASOE, Danish Meteorological Institute, Scientific Report 92-1, Copenhagen, 1992.

Pelon, J. and G. Megie, Ozone monitoring in the troposphere and lower stratosphere: evaluation and operation of a ground based lidar station, J. Geophys. Res., 87, 4947-4955, 1982.

Russell, P.B. and P. Hamill, Spatial variation of stratospheric aerosol acidity and model refractive index: implications of recent results, J. Atmos. Sci., 41, 1781-1790, 1984

Russell, P.B., T.J. Swissler and M.P. McCormick, Methodology for error analysis and simulation of lidar aerosol measurements, Appl. Opt., 18, 3783-3797, 1979.

Sheridan, P.J., R.C. Schnell, D.J. Hofmann and T. Deshler, Electron microscope of Mt. Pinatubo aerosol layers over Laramie, Wyoming during Summer 1991, Geophys. Res. Lett., 19, 2, 199-202, 1992.

A. D'Altorio and G. Visconti, Dipartimento di Fisica, Università de L'Aquila, via Vetoio, 67010 Coppito L'Aquila, Italy.
F. Masci, V. Rizi and E. Boschi, Istituto Nazionale di Geofisica, via Di Vigna Murata 605, 00143 Roma, Italy.